Traffic Signal Timing and Trajectory Optimization in a Mixed Autonomy Traffic Stream

Mehrdad Tajalli, *Member, IEEE*, and Ali Hajbabaie, *Member, IEEE*

***Abstract*— This study introduces a methodology for cooperative signal timing and trajectory optimization at intersections with a mix of connected automated vehicles (CAVs) and human-driven vehicles (HVs). We represent joint signal timing and trajectory control as a mixed-integer non-linear program, which is computationally complex. The developed methodology provides a balance between computational efficiency and solution quality by (a) linearizing the nonlinear constraints and reformulating the problem with a tight convex hull of the mixed-integer solutions and (b) decomposing the intersection-level program into several lane-level programs. Hence, a unique controller jointly optimizes the trajectories of CAVs on a lane and the signal timing parameters associated with that lane. This setting will allow finding near-optimal solutions with small duality gaps for complex intersections with different demand levels. Case study results show that the proposed methodology finds solutions efficiently with at most 0.1% duality gap. We compared the developed methodology with an existing signal timing and trajectory control approach and found 13% to 41% reduction in average travel time and 1% to 31% reduction in fuel consumption under different scenarios.**

***Index Terms*— Signal timing, trajectory optimization, connected and automated vehicles, Lagrangian relaxation.**

I. Introduction

PAST research shows that optimizing the trajectory of connected automated vehicles (CAVs) and the timing of traffic lights at signalized intersections offers a great potential to improve traffic operations [1]–[5]. Joint CAV trajectory and signal timing optimization helps plan the arrival time of vehicles to the intersection more accurately to utilize green durations more efficiently. Therefore, the number of stops, fuel consumption, and travel delay at intersections will be reduced significantly. However, the cooperation between a signal controller and approaching vehicles requires an extensive amount of communication and computational power [6]. It is not likely that a signal controller can handle all the required computations. In fact, previous studies show the effectiveness of signal timing and trajectory optimization (a) in intersections with simple layouts (e.g., one-way streets [2], [7], or no turning movements [8]), (b) under low traffic volumes [2], [7]–[9], or (c) using simplifying or restrictive assumptions (e.g., using first-order traffic flow model to update trajectory of CAVs [4], [10] or optimizing the trajectory of a portion of CAVs [1]). Approximation methods and heuristic algorithms are also used to solve the problem in more complex conditions; however, at the expense of sacrificing the quality of the solutions [11], [12].

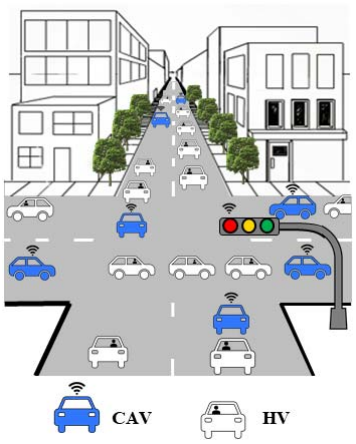

Fig. 1. Connected signal controller interacting with CAVs and HVs.

This article presents a methodology for joint CAV trajectory and signal timing optimization at signalized intersections that provides a balance between computational efficiency and solution quality. As Fig. 1 shows, the methodology is designed for a mixed traffic stream of CAVs and HVs, where the movement of CAVs is controlled centrally and communicated with them through a vehicle-to-infrastructure communication system at the signalized intersection. The methodology requires the initial location and speed of all vehicles (CAVs and HVs) in the vicinity of the intersection and predicts the location of HVs over a planning horizon using car following concepts. The movement of HVs are not optimized. We assume that either all vehicles are connected (just to collect vehicle location and speed), or the intersection is equipped with detectors (e.g., radar units or video cameras) that can provide the location and speed of vehicles. Note that the proposed algorithm works if HVs do not send information to the signal controller as long as detectors are available to collect the required data. This study formulates the joint optimization as a mixed-integer nonlinear program, whose objective reduces the total travel time and speed variance at the intersection. The decision variables are the acceleration rates of CAVs and signal timing parameters. The interaction between HVs and CAVs is incorporated into the optimization problem using a linear car-following model

Manuscript received 17 July 2020; revised 8 December 2020; accepted 3 February 2021. Date of publication 18 February 2021; date of current version 8 July 2022. The Associate Editor for this article was H. A. Rakha. *(Corresponding author: Ali Hajbabaie.)*

The authors are with the Department of Civil, Construction, and Environmental Engineering, North Carolina State University, Raleigh, NC 27695 USA (e-mail: mtajall@ncsu.edu; ahajbab@ncsu.edu).

Digital Object Identifier 10.1109/TITS.2021.3058193

developed by Helly [13]. We modified the linear model to become responsive to traffic lights by incorporating signal timing parameters. The signal timing parameters are optimized through a cycle- and phase-free plan that satisfies the minimum and maximum green constraints in addition to yellow time interval.

The signal timing and trajectory optimization (STTO) problem is complex, especially with the presence of human-driven vehicles, and there is a need to develop computationally efficient algorithms to find near-optimal solutions. Previous studies showed that there is a trade-off between the computational efficiency and optimality of results. This study introduces a solution technique that reduces the complexity of the STTO problem using Lagrangian relaxation technique to decompose the intersection-level signal timing and trajectory optimization problem into several lane-level optimization sub-problems, where a controller optimizes the signal timing parameters and trajectories of CAVs at each lane of an intersection, separately. As a result, STTO can be extended to more complex intersection layouts with high demand levels. In addition, a problem reformulation is proposed using maximal clique sets based on intersection conflict graph to tighten the convex hull of the mixed-integer feasible area and therefore, improve the convergence properties of Lagrangian relaxation technique, which reduces the optimality gap. The near-optimal intersection-level signal timing parameters and CAV trajectories are found through a consensus process between all controllers at the intersection. Furthermore, we propose a simple optimization problem to provide a feasible solution for signal timing plans. Therefore, finding a feasible and high-quality solution is possible without the mentioned restrictive assumptions.

In the remainder of this article, relevant literature is reviewed. The problem formulation is discussed next. Then, the solution technique, including the problem reformulation and Lagrangian relaxation technique is detailed. The result of applying the proposed algorithm to a case study will be provided next, and finally concluding remarks are presented.

II. Background

A. Trajectory Planning at Intersections

Optimizing the trajectory of CAVs at signalized intersections with an advanced knowledge of signal phasing and timing (SPaT) information improves traffic safety, mobility, and fuel consumption efficiency [14]–[17]. The national highway traffic safety administration (NHTSA) reported that SPaT broadcasts are capable of reducing red-light violations and energy consumption by 90% and 35%, respectively [18]. Moreover, vehicle trajectories can be planned with the goal of avoiding stops at an intersection and minimizing fuel consumption. Xia *et al.* [19] showed that a 14% reduction in fuel consumption is possible as a result of an advisory speed system experiment at a fixed-time signalized intersection. Wei *et al.* [20] showed that optimizing the trajectory of the leading vehicle in a platoon approaching a signalized intersection can effectively manage the traffic congestion and increase the capacity of the intersection. When all vehicles are autonomous, controlling the trajectory of CAVs in a signal-free intersection provides the opportunity to achieve the highest capacity of the intersection while maintaining safety by preventing collision between vehicles [21]–[24]. For instance, Mirheli *et al.* [25] showed that the total travel time at a signal-free intersection with 100% CAVs could be reduced up to by 70.5% in comparison with optimized fully actuated signal timing plans.

B. Trajectory and Signal Timing Optimization

Li *et al.* [7] found signal timing and trajectories of CAVs on an intersection of one-way streets, assuming that all vehicles are fully connected and will follow the assigned optimal trajectories. They enumerated all possible signal timing plans and optimized trajectories for each CAV, with the objective of minimizing the average delay. Their proposed approach reduced the average delay by up to 36.9% and increased the throughput by up to 20.2% compared to a fully-actuated signal controller. This approach was not applicable to more complex intersections due to the need to enumerate all possible signal timing plans. Jung *et al.* [8] developed a bi-level program to find traffic signal timing parameters and CAV trajectories at a simple four-leg intersection with only one through link at each direction and only CAVs in traffic stream. An exhaustive search method found the lowest intersection delay at the upper level based on the estimated arrival time of vehicles to the intersection. Then, genetic algorithms determined the trajectories of CAVs at the lower level with the objective of minimizing the total fuel consumption. As a result of this study, the travel time and fuel consumption reduced by up to 12% and 10%, respectively. The combination of the exhaustive search and genetic algorithms might not be efficient enough to solve complex optimization problems. Similarly, Yang *et al.* [2] found signal timing parameters at an isolated intersection with two one-way streets using a branch and bound technique. This study considered three categories of vehicles, including conventional, connected human-driven, and connected and automated vehicles with different market penetration rates. In the upper-level, the total intersection delay was minimized based on the estimated arrival time of vehicles. The trajectories of CAVs were optimized in the lower-level problem for each signal timing plan to maximize their entry speed to the intersection. This study assumed that each platoon leader is a CAV and platoon leaders always arrive at the intersection at the unset of the green signal. The algorithm might not be efficient in complex intersections with high traffic volumes since the trajectories need to be optimized for each set of signal timing parameters identified by the branch and bound algorithm.

Xu *et al.* [9] developed a bi-level program to minimize the total travel time in the upper level and minimize the fuel consumption of each vehicle at the lower level. The signal timing plans were found by enumeration. Then, the optimal trajectory of vehicles for each plan were found by approximating the state and control variables using an interpolating polynomial function. Pourmehrab *et al.* [26] proposed a methodology to adjust the existing signal timing plans based on vehicles arrival time to maximize the utilization of green time. In addition,

trajectory of leading automated vehicles is optimized to minimize the travel time delay. However, this study mainly focused on the feasibility of the signal timing plans rather than their optimality (adjusted the signal timing parameters based on a set of defined rules to find feasible coordination with optimized trajectory). The signal timing control strategy was to extend the signal or switched it to another phase repeatedly until finding a combination that provides arrival on green. In contrast, our proposed approach jointly optimizes signal timing parameters and vehicle trajectories, which leads to more efficient traffic operations.

The enumerative methods such as the ones described in previous studies become ineffective when the intersection layout is complex, the number of phases increases, or the demand level is high. Therefore, some studies proposed heuristics or considered simplified assumptions to solve the signal timing and trajectory optimization problem efficiently. For instance, Feng *et al.* [27] developed a joint optimization method for signal timing and trajectory of platooning CAVs. They divided the signal phases into several stages and used a dynamic programming method to find the signal timing parameters at each stage. The proposed approach could find optimal solutions analytically with the assumption that the platoon leader arrives at the intersection stop bar exactly at the beginning of the green time interval. However, this assumption may limit the choices of signal timing plans in the dynamic programming framework, especially when platoon leaders are not CAVs. Moreover, the effectiveness of the proposed method for high traffic volume was not clear since the study showed the performance results for simple scenarios, where the traffic volume was very low. The result of this study showed that the joint optimization of signal timing and trajectory of platoon leaders reduced vehicle delay and CO_2 emission by up to 24% and 13.8%, respectively. Guo *et al.* [3] proposed a two-step approach to optimize signal timing and trajectory of CAVs. In the first step, the signal timing parameters were found to minimize the intersection delay. In the second step, the optimal trajectories were designed for the planned signal timings. The signal timing parameters were found by dynamic programming, and the effect of each signal plan on trajectories was evaluated through a shooting heuristic, iteratively. Shooting heuristic was shown to estimate high-quality trajectories for CAVs. However, the feasibility of this approach is limited to intersections with links that are long enough to let a vehicle select an appropriate maneuver. In addition, the existence of long queue at the intersection yields finding infeasible solutions by the shooting heuristic.

Yu *et al.* [1] optimized signal timing parameters such as phase sequence, green start time, duration of each phase, and the cycle length at an isolated intersection. Besides, they optimized arrival time of vehicles and lane changing decisions in a four-leg intersection with through, right-turn, and left-turn movements. This study utilized a planning horizon procedure to solve an MILP problem. However, it assumed that (1) all vehicles were CAVs and (2) the vehicles that were in the same lane passing through the intersection in the same cycle were in the same platoon. As a result, they only optimized the trajectory (arrival time) of the leading vehicle, and other following vehicles followed the leader with a car-following model. In addition, they assumed that all vehicles arrived the intersection with their desired speed and no queue existed at the intersection. These assumptions restrict the application of the proposed methodology to low CAV market penetration rate levels. Li *et al.* [28] optimized trajectory of electric vehicles in combination with signal timing plans for an arterial street with multiple intersections. The objective of this study was to minimize the traffic delay by optimizing signal timings and save the energy of electric vehicles by optimizing their trajectory. To solve this complex optimization problem, a hybrid heuristic technique comprised of genetic algorithm and particle swarm optimization was utilized to generate feasible signal timing plans and consequently evaluate optimal trajectories for that signal. The study reduced the problem complexity by considering optimal trajectories from each vehicle perspective without coordination among them. Therefore, the solution may not improve system-level performance.

Li and Zhou [4] optimized signal timings and trajectories of CSVs in a mixed environment with human-driven vehicles. They reduced the complexity of the problem by representing the traffic dynamic and signal timing constraints within a phase-time traffic hyper-network. However, this representation required a first-order heterogeneous traffic model. Although their proposed approach allows studying large-scale networks, its accuracy for operational purposes is not as high as the proposed model in our study that uses car-following models. The performance of the phase-time traffic hyper-network approach is not clear when a second-order traffic flow or microscopic car following model is considered, where the complexity of the problem will increase significantly. In a similar study, Li *et al.* [10] used Lagrangian relaxation technique to solve the signal timing and routing problem in a transportation network. The Lagrangian relaxation was used to relax the link capacity constraints and to decompose the optimization program into routing guidance and signal optimization subproblems. However, optimizing vehicles' routes is different than trajectory optimization since route optimization does not control the location of vehicles over short time interval. Although the Lagrangian relaxation technique reduced the complexity of the proposed problem, the reported optimality gaps in this study was as high as 30%, which lead to suboptimal solutions.

C. Summary of the Literature and Contribution of the Paper

The signal timing and trajectory optimization problem is complex and there is a need to develop algorithms providing a balance between computational complexity and solution quality. Previous studies showed that there is a trade-off between the computational efficiency and solution quality, where more efficient algorithms are associated with more simplifying assumptions. The contributions of this study are three-fold: 1) this study introduces a solution technique that provides a balance between computational efficiency and solution quality: it reduces the computational complexity of STTO without significantly sacrificing the quality of the solution. We achieved this balance by developing an efficient solution

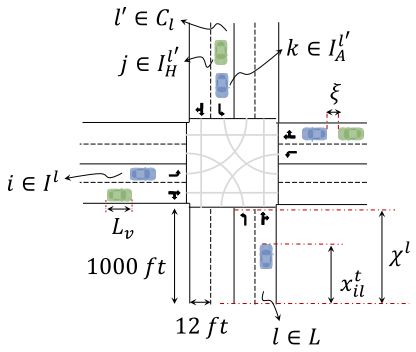

Fig. 2. Defined sets and parameters in STTO problem.

technique using Lagrangian relaxation method to decompose a centralized STTO problem into several lane-level optimization sub-problems. Therefore, intersections with various layouts and different demand levels can be analyzed; 2) we reduced the optimality gap of the proposed Lagrangian relaxation approach so that the solutions that it finds are close to the optimal solutions. We did so by proposing a problem reformulation using maximal clique sets to tighten the convex hull of mixed-integer feasible region. As a result, we improve the convergence property of Lagrangian relaxation technique for STTO problem and ensure finding near optimal solutions efficiently with reduced duality gap; 3) the proposed algorithm does not require the following simplifying assumptions: a) fleet of all automated vehicles, b) forcing vehicles to move in a platoon, c) arriving at the intersection with the desired speed, or d) no initial queue existing at the intersection during red phases. Therefore, the effect of joint signal timing and trajectory optimization of CAVs can be studied in a mixed autonomy environment with various market penetration rates of CAVs.

III. Problem Formulation

This study optimizes the trajectory of all CAVs and signal timing parameters cooperatively. The initial location and speed of human-driven vehicles are assumed to be known by the infrastructure through radar units, video detectors, or connectivity. We define L as the set of all lanes at an intersection and I as the set of all vehicles at the intersection neighborhood. Moreover, I^l, I_A^l, and I_H^l represent the sets of all vehicles, CAVs, and HVs on lane $l \in L$, respectively. We define C_l as the set of all lanes conflicting with lane $l \in L$. Fig. 2 shows the defined sets in an isolated intersection.

We define T_s and T_t as the set of signal timing and trajectory optimization time steps, respectively. Note that vehicle trajectory and signal timing update time steps (ΔT_t and ΔT_s, respectively) are different. The trajectory are updated more frequently than signal timing parameters to take into account the uncertainty in driver behaviors and capture any differences between the predicted and actual vehicle trajectory. Equations (1) shows the relation between these two time steps. The $\lfloor\rfloor$ operator rounds down the corresponding argument inside it.

$$p = \left\lfloor t \times \frac{\Delta T_t}{\Delta T_s} \right\rfloor \quad t \in T_t,\ \ p \in T_s \tag{1}$$

TABLE I

Definition of Sets, Decision Variables, and Parameters

Sets:	
T_t	set of all time steps for trajectory updates
T_s	set of all time steps for signal timing updates
L	set of all lane groups at the intersection
I^l	set of all vehicles on lane $l \in L$
I_A^l	set of all CAVs on lane $l \in L$
I_H^l	set of all HVs on lane $l \in L$
C_l	set of all lanes conflicting with lane $l \in L$
Decision Variables:	
a_{il}^t	the acceleration of vehicle $i \in I_l$ on lane $l \in L$ at time $t \in T_t$
g_l^p	a binary variable for green signal on lane $l \in L$ at time $p \in T_s$
y_l^p	a binary variable for yellow signal on lane $l \in L$ at time $p \in T_s$
State Variables:	
x_{il}^t	the relative distance of vehicle $i \in I_l$ at time step $t \in T_t$ from the beginning of lane $l \in L$
v_{il}^t	the speed of vehicle $i \in I_l$ on lane $l \in L$ at time step $t \in T_t$
Parameters:	
v'	maximum speed
v	minimum speed
σ'	maximum acceleration
σ	minimum acceleration
χ^l	the relative location of intersection stop bar from the beginning of lane $l \in L$
w_l	weight factor
L_v	the length of vehicle
ξ	desired safety distance between vehicles
τ_H	the reaction time of HVs
τ_A	the reaction time of CAVs
β	weight factor in the objective function
ω_l'	maximum green time for lane $l \in L$
ω_l	minimum green time for lane $l \in L$
ψ	yellow time interval
M	a very large value

The status of the signal timing variables including green time g_l^p and yellow time y_l^p on lane $l \in L$ and time-step $p \in T_s$ will be optimized based on information on location x_{il}^t and speed v_{il}^t of vehicle $i \in I^l$ approaching the intersection on lane $l \in L$ at time-step $t \in T_t$. The acceleration rate a_{il}^t of vehicle $i \in I_A^l$ at time $t \in T_t$ is also the control variable in motion planning of CAVs. Table I provides a detailed definition of variables, sets, and parameters used in the problem formulation.

A. Objective Function

The objective function of STTO is shown in (2) with two terms. The first term maximizes the distance of each vehicle from the beginning of lane $l \in L$, where vehicle $i \in I^l$ is located on (see Fig. 2) [29], [30]. Weight factor w_{il} for vehicle $i \in I_l$ on lane $l \in L$ is multiplied by the first term of the objective function to avoid constantly serving approaches with higher demand and preventing queue buildup at the minor direction of the intersection. We set the value of this weight equal to the current delay that each vehicle has experienced after entering the intersection vicinity (i.e. free flow travel time minus actual travel time). Therefore, a higher priority will be assigned to vehicles on a lane with higher experienced delays. Note that the weight factor is fixed over the planning horizon. The second term of the objective function smoothens the motion of CAVs by minimizing the

difference of speeds of each CAVs between two consecutive time steps. Tajalli and Hajbabaie [14] showed that minimizing the difference in speeds yields to a smaller number of stops at intersections. The weight factor $\beta \in (0, 1)$ is an input to the optimization program to provide a desired balance among the two terms of the objective function. A higher value of β gives more priority to the first term and a lower value of β provide a higher priority to the second term of the objective function.

$$f = \underset{\boldsymbol{a}}{\text{Max}} \Big(\beta \sum\nolimits_{t\in T_t} \sum\nolimits_{l\in L} \sum\nolimits_{i\in I^l} w_{il} x_{il}^t - (1-\beta) \sum\nolimits_{t\in T_t} \sum\nolimits_{l\in L} \sum\nolimits_{i\in I_A^l} \left| v_{il}^{t+1} - v_{il}^t \right| \Big) \quad (2)$$

B. Constraints

The speed and position of all vehicle are updated based on basic equations of motion, as shown in constraints (3) and (4).

$$v_{il}^{t+1} = v_{il}^t + a_{il}^t \Delta T_t \quad \forall i \in I^l,\ l \in L,\ t \in T_t \quad (3)$$

$$x_{il}^{t+1} = x_{il}^t + v_{il}^t \Delta T_t + \frac{1}{2} a_{il}^t \Delta T_t^2 \quad \forall i \in I^l,\ l \in L,\ t \in T_t \quad (4)$$

1) Car Following Constraints: The estimated location and speed of HVs are needed for optimizing the signal timing parameters and trajectory of CAVs. Hence, the future trajectory of HVs are predicted based on a car-following behavior. This study considered the linear car-following model developed by Helly (1959). This car-following model is used in modeling adaptive and cooperative adaptive cruise control systems [31], [32]. Furthermore, Panwai and Dia (2005) showed an appropriate fit of Helly's car following model to real-world traffic data. Although the nature of human driving is stochastic, a deterministic car-following model works appropriately in our approach. The reason is that the initial location of vehicles is observed from the network every 0.5 seconds by the receding horizon control methodology, which will be explained in the methodology section. The followers respond to both relative speed and distance from their preceding vehicle in this car following model, see Equations (5) for calculation of the acceleration rate. Parameters α_1 and α_2 are fixed, have positive values, and should be within the ranges of [0.17, 1.3] and $[\frac{1}{4}\alpha_1, \frac{1}{2}\alpha_1]$, respectively [34], [35].

$$a'^t_{il} = \alpha_1 \left(v_{i-1,l}^t - v_{il}^t\right) + \alpha_2 \left(\left(x_{i-1,l}^t - x_{il}^t - L_v\right) - \xi - \tau_H v_{il}^t\right) \quad \forall i \in I_H^l,\ l \in L,\ t \in T_t \quad (5)$$

The first term in Equations (5) considers the relative speed between the leading and following vehicles. A positive speed difference (i.e., leader travels at a higher speed) results in a positive acceleration rate for the follower, while a negative speed difference forces the follower to decelerate. The second term takes into account the relative distance between successive vehicles.

We enhance the car-following model to account for traffic signals so that a vehicle decelerates when approaching a red signal. The traffic light is considered as a virtual vehicle with either zero speed at the stop bar (for a red signal) or max speed for from the intersection (for a green signal). Equations (6) show how a vehicle's acceleration rate is updated while approaching the stop bar. Note that when the signal is red, $g_l^p = 0$, the virtual stopped vehicle is located at the intersection stop bar χ^l and there would be desired safety distance ξ between the vehicle and the intersection stop bar. However, when the traffic light is green, the location of preceding virtual vehicle changes to a far distance from the following vehicle and the desired safety distance to the intersection stop bar will be reduced to zero. Moreover, it should be noted that the connection between vehicles and traffic light is only needed when vehicles are before the intersection stop bar with $x_{il}^t \le \chi^l$. Equations (6) should become inactive after a CAV passes the intersection. Multiplying signal timing variable g_l^p with big coefficient M in the second term of Equations (6) moves the virtual car to a very long distance from the following vehicle when signal is green. As such, the vehicle does not react to it anymore.

Binary variable γ_{il}^t is introduced in Equations (6) to relax the connection between the traffic light and vehicles after they pass the intersection stop bar ($x_{il}^t > \chi^l$). Variable γ_{il}^t becomes zero when the vehicle is upstream of the intersection stop bar and becomes one when the vehicle has passed the intersection stop bar. Equations (7) defines the value of γ_{il}^t for vehicle $i \in I^l$ on lane $l \in L$ at time step $t \in T_t$.

$$a''^t_{il} = \alpha_1 \left(g_l^p v' - v_{il}^t\right) + \alpha_2 \left(\left(\chi^l + M g_l^p - x_{il}^t\right) - (1 - g_l^p)\xi\right) + M\gamma_{il}^t \quad \forall i \in I_H^l,\ l \in L;\ t \in T_t,\ p \in T_s \quad (6)$$

$$\gamma_{il}^t = \begin{cases} 0 & \text{if } x_{il}^t \le \chi^l \\ 1 & \text{otherwise} \end{cases} \quad \forall i \in I^l,\ l \in L,\ t \in T_t \quad (7)$$

The linear car-following model presented by Equations (5) and (6) does not limit the acceleration rate and speed between minimum and maximum values. As a result, we formulate the car following model based on a max-min function, as shown in Equations (8). This formulation is a complete form of the proposed car-following model that describes situations such as moving in free-flow condition, following other vehicles in stationary and non-stationary conditions, and approaching slow or standing vehicles and red signals.

$$a_{il}^t = \max\left(\sigma, \frac{v - v_{il}^t}{\Delta T_t}, \min\left(\sigma', \frac{v' - v_{il}^t}{\Delta T_t}, \alpha_1 \left(g_l^p v' - v_{il}^t\right) + \alpha_2 \left(\left(\chi^l + M g_l^p - x_{il}^t\right) - (1 - g_l^p)\xi\right), a'^t_{il}, a''^t_{il}\right)\right) \quad \forall i \in I_H^l,\ l \in L,\ t \in T_t, p \in T_s \quad (8)$$

2) CAV Motion Constraints: Objective function (2) smoothens the trajectory of CAVs to prevent frequent stops at the intersection. Constraints (9) ensures a safe distance between a CAV and its preceding vehicle. The distance between two consecutive vehicles is a function of desired safety distance ξ, average vehicle length L_v, and distance $\tau_A v_{il}^t$ that can be passed within the reaction time of the following vehicle. Parameter τ_A represent the reaction time for CAVs.

$$x_{i-1,l}^t - x_{il}^t \ge \xi + L_v + \tau_A v_{il}^t \quad \forall i \in I_A^l,\ l \in L,\ t \in T_t \quad (9)$$

Constraints (10) is used to prevent a CAV from entering the intersection area when the signal is not green. When a CAV has not arrived at the intersection and the signal is red, the distance

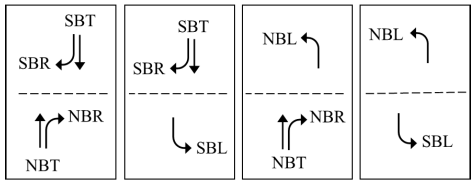

Fig. 3. The allowed movements for northbound and southbound approaches.

between the vehicle and intersection stop bar should be greater than or equal to a safety distance, as shown on the right-hand side of constraints (10). The safety distance is a function of the maximum distance $\Delta T_t v_{il}^t$ that a vehicle can travel in one time step with its current speed at time $t \in T_t$. These constraints need to become inactive when either the signal is green, or the vehicle has passed the stop bar. Therefore, variables g_l^p and γ_{il}^t are multiplied to a large number (M) to ensure that constraints (10) are always satisfied when either the signal is green, or the vehicle has passed the stop bar.

$$\chi^l - x_{il}^t \geq \Delta T_t v_{il}^t - M g_l^p - M \gamma_{il}^t \quad \forall i \in I_A^l,\ l \in L,\ t \in T_t,\ p \in T_s \tag{10}$$

Constraints (11) and (12) limit the acceleration and speed of CAVs between allowed ranges, respectively.

$$\sigma \leq a_{il}^t \leq \sigma' \quad \forall i \in I_A^l,\ l \in L,\ t \in T_t \tag{11}$$

$$\upsilon \leq v_{il}^t \leq \upsilon' \quad \forall i \in I_A^l,\ l \in L,\ t \in T_t \tag{12}$$

3) Signal Timing Constraints: The signal timings are assumed to be cycle- and phase-free; however, restricted to non-conflicting movements. Fig. 3 shows all allowed movements for northbound and southbound approaches, as an example. We assume that through and right-turn movements can go on the same lane.

Several constraints are considered to prevent collisions between vehicles on conflicting movements. The signal timing decision variables g_l^p and y_l^p respectively take on the value of one when the traffic light serving lane $l \in L$ at time step $p \in T_s$ is green or yellow. Otherwise, both g_l^p and y_l^p take on the value of zero simultaneously, which means that the signal is red. Constraints (13) ensure that no pair of conflicting movements can receive a non-red traffic light at time step $p \in T_s$. In other words, the traffic signals serving lanes with conflicting movements can be red at the same time, but only one of them can be either green or yellow at a time. In addition, constraints (13) prevent the signal status of a lane to be green and yellow at the same time.

$$g_l^p + g_{l'}^p + y_l^p + y_{l'}^p \leq 1 \quad \forall l \in L,\ l' \in C_l,\ p \in T_s \tag{13}$$

Constraints (14) ensure that green time assigned to a lane is less than or equal to maximum green time ω_l'. Constraints (15) ensure that the green time duration for lane group $l \in L$ is greater than or equal to minimum green time ω_l.

$$\sum\nolimits_{j=p}^{p+\omega_l'} g_l^j \leq \omega_l' \quad \forall l \in L,\ p \in T_s \tag{14}$$

$$\sum\nolimits_{j=p+1}^{p+\omega_l} g_l^j \geq \left(g_l^{p+1} - g_l^p\right) \omega_l \quad \forall l \in L,\ p \in T_s \tag{15}$$

Constraints (16) define the duration of yellow time, and constraints (17) make sure that the signal switches from green to yellow at the end of the green time interval. Parameter $\mathcal{Y}$ is the yellow time interval. Constraints (18) ensures the integrality of signal timing variables.

$$\sum\nolimits_{j=p}^{p+Y} y_l^j \leq \mathcal{Y} \quad \forall l \in L,\ p \in T_s \tag{16}$$

$$\sum\nolimits_{j=p+1}^{p+Y} y_l^j \geq \left(g_l^p - g_l^{p+1}\right) \mathcal{Y} \quad \forall l \in L,\ p \in T_s \tag{17}$$

$$g_l^p, y_l^p \in \{0, 1\} \quad \forall l \in L,\ p \in T_s \tag{18}$$

To summarize, signal timing and trajectory optimization problem can be shown as follows:

$$STTO:$$

$$f = \max_{\boldsymbol{a}} \left(\beta \sum\nolimits_{t \in T_t} \sum\nolimits_{l \in L} \sum\nolimits_{i \in I^l} w_{il} x_{il}^t - (1-\beta) \sum\nolimits_{t \in T_t} \times \sum\nolimits_{l \in L} \sum\nolimits_{i \in I_A^l} \left| v_{il}^{t+1} - v_{il}^t \right| \right)$$

s.t.

$$(3)-(4), (8), (9)-(12), (14)-(18)$$

IV. Methodology

The proposed formulation is a mixed-integer nonlinear program. This optimization program is intractable and cannot be solved efficiently due to the presence of nonlinear constraints and binary variables. We first linearize the objective function (2), car-following model (8), and conditional constraints to reduce the computational complexity of the proposed formulation. We use the Lagrangian relaxation technique to decompose the intersection-level problem into several lane-level sub-problems with reduced computational complexity and the possibility of allocating one controller to each of them. The controllers will reach a consensus on signal timing parameters and CAV trajectories through sharing Lagrangian multipliers to ensure that a near-optimal solution is found when conflict avoidance constraints (13) are satisfied.

A. Linearization

The second term of the objective function (2) contains an absolute value function, which is convex but nonlinear. We introduce two auxiliary non-negative variables z_i^t and u_i^t for each vehicle $i \in I_A^l$ at time step $t \in T_t$ to linearize the absolute value function. Constraints (20) and (21) are added to the original problem to enforce that the difference of z_i^t and u_i^t equals the terms in the absolute value function. The linear form of objective function (2) is shown in (19), where the sum of auxiliary variables is minimized.

$$\max_{\boldsymbol{a}} \left(\beta \sum\nolimits_{t \in T_t} \sum\nolimits_{l \in L} \sum\nolimits_{i \in I^l} w_{il} x_{il}^t - (1-\beta) \sum\nolimits_{t \in T_t} \sum\nolimits_{l \in L} \sum\nolimits_{i \in I_A^l} \left(z_{il}^t + u_{il}^t\right)\right) \tag{19}$$

$$z_{il}^t - u_{il}^t = v_{il}^{t+1} - v_{il}^t \quad \forall i \in I^l,\ l \in L,\ t \in T_t \tag{20}$$

$$z_{il}^t \geq 0, u_{il}^t \geq 0 \quad \forall i \in I^l,\ l \in L,\ t \in T_t \tag{21}$$

Constraints (8) are nonlinear due to the existence of a max-min function. We provide a linear form of these constraints

by converting the equality constraints to several inequalities and adding a penalty term to the objective function. Auxiliary variable $b_{il}^t \in R^n$ is introduced to represent the min part of the max-min function (8). Note that b_{il}^t has the same unit as acceleration (ft/s^2) and can take both positive and negative values. As constraints (22)-(25) show, the min part of constraints (8) are represented by less than or equal inequalities.

$$b_{il}^t \leq \sigma' \quad \forall i \in I_H^l,\ l \in L,\ t \in T_t \tag{22}$$

$$b_{il}^t \leq \frac{v' - v_{il}^t}{\Delta T_t} \quad \forall i \in I_H^l,\ l \in L,\ t \in T_t \tag{23}$$

$$b_{il}^t \leq a'^t_{il} \quad \forall i \in I_H^l,\ l \in L,\ t \in T_t \tag{24}$$

$$b_{il}^t \leq a''^t_{il} \quad \forall i \in I_H^l,\ l \in L,\ t \in T_t,\ p \in T_s \tag{25}$$

Constraints (26)-(27) relax the max part of function (8), which is represented by greater than or equal inequalities. Constraints (28) ensure that a_{il}^t is greater than or equal to b_{il}^t from the relaxed min function.

$$a_{il}^t \geq \sigma \quad \forall i \in I_H^l,\ l \in L,\ t \in T_t \tag{26}$$

$$a_{il}^t \geq \frac{v - v_{il}^t}{\Delta T_t} \quad \forall i \in I_H^l,\ l \in L,\ t \in T_t \tag{27}$$

$$a_{il}^t \geq b_{il}^t \quad \forall i \in I_H^l,\ l \in L,\ t \in T_t \tag{28}$$

The proposed linearization (22)-(28) is loose and cannot equivalently represent the max-min form of (8). To fix this issue, we penalize the non-negative difference $a_{il}^t - b_{il}^t \geq 0$ with big penalty coefficient M in the objective function. The new objective function is shown by (29) that pushes b_{il}^t towards a_{il}^t.

$$\max_{\boldsymbol{a}} \Big(\beta \sum\nolimits_{t\in T_t} \sum\nolimits_{l\in L} \sum\nolimits_{i\in I^l} w_{il} x_{il}^t - (1-\beta) \sum\nolimits_{t\in T_t} \sum\nolimits_{l\in L} \sum\nolimits_{i\in I_A^l} \left| v_{il}^{t+1} - v_{il}^t \right| - M \sum\nolimits_{t\in T_t} \sum\nolimits_{l\in L} \sum\nolimits_{i\in I_H^l} \left(a_{il}^t - b_{il}^t\right)\Big) \tag{29}$$

Constraints (7) are nonlinear due to the if-else condition. The Big-M method allows linearizing the constraints as shown in (30) and (31). If γ_{il}^t takes the value of 0, constraints (30) show that the location of vehicle $i \in I^l$ is before the location of the intersection stop bar on lane $l \in L$ at time $t \in T_t$. However, when γ_{il}^t takes the value of one, constraints (31) ensure that vehicle's location is after the intersection stop bar.

$$x_{il}^t - \chi^l \leq M\gamma_{il}^t \quad \forall i \in I^l,\ l \in L,\ t \in T_t \tag{30}$$

$$x_{il}^t - \chi^l \geq M(\gamma_{il}^t - 1) \quad \forall i \in I^l,\ l \in L,\ t \in T_t \tag{31}$$

B. Lagrangian Relaxation

The linearization techniques described in the previous section converts a mixed-integer nonlinear problem (MINLP) to a mixed-integer linear problem (MILP). Although this conversion reduces the complexity of the problem, the existence of integer signal timing and other variables makes the problem still intractable and difficult to solve. We develop a Lagrangian relaxation technique that decomposes the problem into several lane-level optimization sub-problems, where the optimal signal timing and vehicles trajectories on each lane of the intersection are found separately in parallel. However,

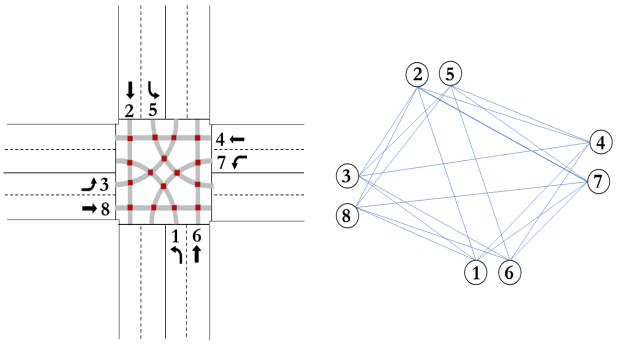

Fig. 4. Conflict graph for a four-leg intersection with through and left-turn movements.

Lagrangian relaxation might not hold a strong duality for MILPs [36], [37]. Hence, we reformulate the problem with a superior solution space structure to overcome this issue. Then, a simple optimization problem is introduced to ensure having a feasible solution for signal timing plans.

1) Problem Reformulation: Pairwise constraints (13) are the only common constraints between the lanes that prevent conflicting movements to receive a non-red signal at the same time. Relaxing these constraints and adding them to the objective function with Lagrangian multipliers leads to a lane-level decomposition. The Lagrangian relaxation provides an upper-bound to the optimal solution of non-convex signal timing and trajectory optimization problem based on the weak duality theory. The feasible convex polyhedron provided by the pairwise constraints has non-integer extreme points due to the weak structure of pairwise constraints [38]. In other words, there are too many constraints associated with pairwise constraints (13), hence the continuous linear relaxation contains many fractions in most of the cases [38]. Therefore, there is no guarantee that the Lagrangian relaxation converges to the desired integer solutions with non-zero duality gap [37]. Finding hyperplanes that define the convex hull of integer solutions helps overcome finding infeasible solutions after the relaxation in addition to satisfying the pairwise constraints.

Pairwise conflicting constraints (13) can be represented by an undirected conflict graph $G = (N, E)$ that contains edge $\{i, j\} \in E$ if and only if two nodes within a pair of binary nodes $i, j \in N$ cannot be selected at the same time (i.e., two conflicting movements). In other words, E is the edge between two binary nodes when at most one of them can take the value one in the solution of MILP. Fig. 4 shows the conflict graph for an intersection with four approaches and eight lanes containing through and left-turn movements. The nodes of the graph are signal heads associated with lane $l \in L$, and each edge represents a pairwise conflict constraints represented by (13).

The graph shown in Fig. 4 represents all conflicts at intersections with exclusive left-turn movements, assuming the right-turn movements are operated with the through movements. Pairwise conflicting constraints (13) are a special case of a more powerful set of constraints called cliques [39]. A clique is a set of several mutually conflicting movements that at most one of them can receive a non-red signal at a time in this

study. We define clique $k \in K$ as a set of mutually connected nodes in the conflict graph G, where K is the set of all possible cliques. Respectively, set C_k represents all members of clique k, where each member is mutually connected in graph G. In order to have set C_k in clique k, it is required that all potential nodes $i, j \in C_k$ be connected to each other through the edges of graph G. For instance, $k = \{8, 6, 7\}$ is a clique for the intersection shown in Fig. 4 since at most one of the movements among $8, 6$, and 7 can get a non-red signal. Multiple pairwise constraints (13) between different movements can be represented in one clique. Hence, it is possible to define a complete set of clique constraints that impose all edge restrictions with a smaller number of constraints. Respectively, we define the maximal clique as a clique that cannot be enlarged by adding any additional node. Let define variable s_l^p as the sum of green g_l^p and yellow y_l^p signal timing variables on lane $l \in L$ and time $p \in T_s$. This is binary because at most one of the green and yellow signal timing status take on the value of one, see constraints (32)-(34).

$$s_l^p = g_l^p + y_l^p \quad \forall l \in L, \ p \in T_s \tag{32}$$

$$\sum\nolimits_{l \in C_k} s_l^p \leq 1 \quad \forall k \in K, \ p \in T_s \tag{33}$$

$$s_l^p \in \{0, 1\} \quad \forall l \in L, \ p \in T_s \tag{34}$$

The intersection graph with exclusive left-turn movements cannot have cliques of a size of larger than four. Therefore, any clique of size four is a maximal clique. In addition, it can be confirmed that the maximal cliques in the intersection conflict graph maintain all the necessary restrictions to prevent two conflicting movements to receive a non-red signal at the same time. Besides, the maximal cliques with size four are facet-defining for the convex hull of all feasible area from pairwise constraints (13) [40]. As a result, the feasible convex hull is tightened and the number of relaxed constraints is reduced significantly. Therefore, the duality gap reduces in Lagrangian relaxation problem.

2) Simplified STTO and Corresponding Dual Formulation: As described in the previous section, constraints (13) are replaced with constraints (32)-(34) to achieve the simplified STTO (SSTTO) as follows.

$$SSTTO:$$

$$f' = \underset{\boldsymbol{a}}{\text{Max}} \Big(\beta \sum\nolimits_{t \in T_t} \sum\nolimits_{l \in L} \sum\nolimits_{i \in I^l} w_l x_{il}^t - (1-\beta) \sum\nolimits_{t \in T_t} \sum\nolimits_{l \in L} \sum\nolimits_{i \in I_A^l} \left(z_i^t + u_i^t\right) - M \sum\nolimits_{t \in T_t} \sum\nolimits_{l \in L} \sum\nolimits_{i \in I_H^l} \left(a_{il}^t - b_{il}^t\right)\Big)$$

s.t.

$$(3)-(4), (9)-(12), (14)-(18), (20)-(28), (30)-(31), (32)-(34) \tag{35}$$

Relaxing complicating constraints (33) decomposes the SSTTO problem into lane-level sub-problems. Therefore, the Lagrangian problem is obtained by dualizing clique constraints (33) as follows:

$$LR-SSTTO:$$

$$L(\boldsymbol{\mu}) = \underset{\boldsymbol{a}}{\text{Max}} \Big(\beta \sum\nolimits_{t \in T_t} \sum\nolimits_{l \in L} \sum\nolimits_{i \in I^l} w_l x_{il}^t - (1-\beta) \sum\nolimits_{t \in T_t} \sum\nolimits_{l \in L} \sum\nolimits_{i \in I_A^l} \left(z_i^t + u_i^t\right) - M \sum\nolimits_{t \in T_t} \sum\nolimits_{l \in L} \sum\nolimits_{i \in I_H^l} \left(a_{i,l}^t - b_{i,l}^t\right) + \sum\nolimits_{p \in T_s} \sum\nolimits_{k \in K} \sum\nolimits_{l \in C_k} \mu_{lk}^p \left(1 - s_l^p\right)\Big)$$

s.t.

$$(3)-(4), (9)-(12), (14)-(18), (20)-(28), (30)-(31), (32), (34) \tag{36}$$

where $\mu_{lk}^p \in R^+$ is the Lagrangian multiplier for lane $l \in C_k$ that belongs to clique $k \in K$ at time step $p \in T_s$. Vector $\boldsymbol{\mu}$ is defined as the vector of all Lagrangian multipliers. Since the objective function and the remaining constraints of problem LR are separable over lanes, the sub-problem for each lane $l \in L$ can be solved separately in parallel when the dual multiplier $\boldsymbol{\mu}$ is available. The values of the dual function $L(\boldsymbol{\mu})$ at dual feasible point $\boldsymbol{\mu}$ are always upper-bounds to the optimal value f'. Hence, the sharpest upper-bound can be found from the optimal value of dual problem (37), which is defined as $\boldsymbol{\mu}^*$.

$$L\left(\boldsymbol{\mu}^*\right) = \min_{\boldsymbol{\mu} \in R} L(\boldsymbol{\mu}) \tag{37}$$

By duality theory, dual problem (37) is always convex. In other words, solving Lagrangian dual problem (37) is equivalent to minimizing a convex piecewise linear function. A function $f : R^n \rightarrow R$ is a piecewise linear convex function if f is attained as the maximum of the finite number of affine functions $f_i : R^n \rightarrow R$. We can use this feature to find the optimal Lagrangian multipliers $\boldsymbol{\mu}$ through the dual cutting plane method.

3) Update Lagrangian Multipliers: The subgradient method is a common approach to solve the Lagrangian dual problem and update the Lagrangian multipliers. However, it suffers from a slow convergence [41], [42]. The subgradient method utilizes the information of only the last iteration to update the Lagrangian multipliers. On the other hand, using the dual cutting plane method helps store the information of all previously found Lagrangian multipliers ($\boldsymbol{\mu^n}$), the optimal Lagrangian relaxation function $L(\boldsymbol{\mu^n})$, and the subgradient $r(\boldsymbol{\mu^n})$ up to iteration n and use them to find the new Lagrangian multiplier $\boldsymbol{\mu^{n+1}}$ at next iterations [43]. The subgradient r_k^p corresponding to each relaxed constraints is found from (38).

$$r_k^p = 1 - \sum\nolimits_{l \in C_k} s_l^t \quad \forall k \in K, \ p \in T_s \tag{38}$$

Based on the definition of subgradient, inequality (39) is satisfied for all $\boldsymbol{\mu}$.

$$L(\boldsymbol{\mu}) \geq L\left(\boldsymbol{\mu^n}\right) + r\left(\boldsymbol{\mu^n}\right)^T \left(\boldsymbol{\mu} - \boldsymbol{\mu^n}\right) \quad \forall \boldsymbol{\mu} \in R^n \tag{39}$$

To update the Lagrangian multiplier, a stabilized version of the cutting plane is introduced as the proximal bundle method [44]. Similar to the cutting plane method, a polyhedral model of dual function (41) is considered in the proximal bundle approach. In addition, a quadratic penalty term is added to the objective function (40) to stabilize the optimal Lagrangian multiplier around the center point $\boldsymbol{\mu_{cp}}$. The center

point is considered as the best Lagrangian multiplier that has been found so far that significantly improves the solutions. Parameter $h \in R^+$ controls the weight of the quadratic term. Solving this optimization problem over iterations provides a sequence of Lagrangian multipliers $\{\boldsymbol{\mu}^{\boldsymbol{n}}\}_{n=1,\ldots,N}$. Iteration N is considered as the last iteration in the cutting plane optimization.

$$DO:$$

$$\min_{\mu \in R} v + \frac{1}{2h} \left\| \boldsymbol{\mu} - \boldsymbol{\mu}_{\mathbf{cp}} \right\|^2 \tag{40}$$

s.t.

$$v \geq L\left(\boldsymbol{\mu}^{\boldsymbol{n}}\right) + r\left(\boldsymbol{\mu}^{\boldsymbol{n}}\right)^T \left(\boldsymbol{\mu} - \boldsymbol{\mu}^{\boldsymbol{n}}\right) \quad n = \{1, \ldots, N\} \tag{41}$$

4) Making Infeasible Solutions Feasible: Solving the Lagrangian relaxation problem iteratively converges to $\boldsymbol{\mu}^*, \boldsymbol{g}^*$, and $\boldsymbol{y}^*$ as the optimal Lagrangian multipliers, green signal status, and yellow signal status, respectively. In addition, it yields the corresponding optimal trajectory of all CAVs. Although reformulating the problem reduces the duality gap to a very small value, the optimal solution of Lagrangian relaxation still may be an infeasible signal timing parameter, that does not satisfy relaxed constraints (33). We introduce a simple optimization problem that finds a good feasible signal timing solution in such conditions. Reformulating constraints (13) with (33) pushes the solution of signal timing variables from Lagrangian relaxation problem to close proximity of the feasible integer values in the convex polyhedron. As a result, there would be no need to change the structure of the Lagrangian relaxation solution. We need to project the final infeasible signal timing solutions to the closest feasible integer point. The complementary optimization problem *FP* is introduced to ensure the feasibility of the solutions from the relaxed problem.

The decision variables in FP are all signal timing variables. In addition, $\mathbf{g}^*$ and $\mathbf{y}^*$ found from the Lagrangian relaxation are inputs. The objective function of the proposed optimization problem minimizes the difference between signal timing variables and the corresponding solutions from the Lagrangian relaxation. In addition, all signal timing constraints, including the relaxed pairwise constraints, are considered in FP. Constraints (43) are also added to the problem, assuming that the optimal signal timing parameters always give non-red signal status to at least two movements at the same time. The optimization problem *FP* is always feasible if the prediction horizon of signal timing T_s is greater than the minimum green time for all approaches of the intersection.

$$FP:$$

$$\min_{g,y \in \{0,1\}} \sum\nolimits_{l \in L} \sum\nolimits_{p \in T_s} \left\| g_l^p - \boldsymbol{g}_l^{*p} \right\|^2 + \left\| y_l^p - \boldsymbol{y}_l^{*p} \right\|^2 \tag{42}$$

s.t.

$$(13) - (18)$$

$$\sum\nolimits_{l \in L} g_l^p + y_l^p \geq 2 \quad \forall l \in L, \;\; p \in T_s \tag{43}$$

5) Receding Horizon Control: The Lagrangian relaxation for finding the optimal signal and trajectory optimization problem is embedded in a receding horizon control (RHC) to take into account the dynamic nature of the problem.

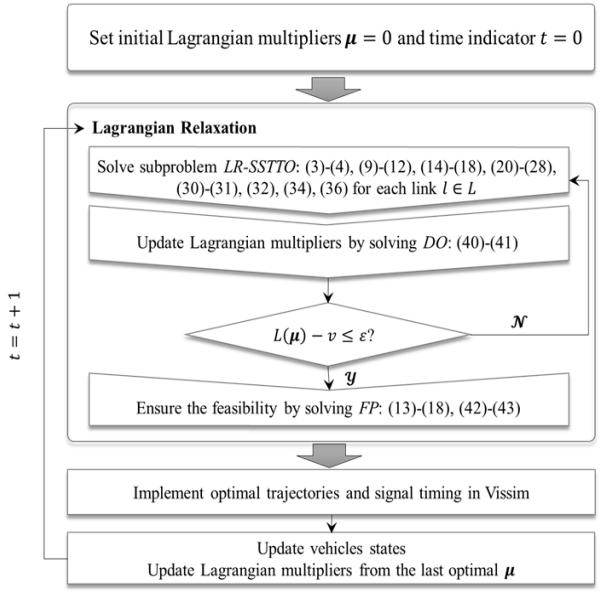

Fig. 5. Lagrangian relaxation procedure embedded in RHC.

Fig. 5 shows the general solution technique framework. First, we initialize the Lagrangian multipliers at time step 0. Then, the *LR-SSTTO* program is solved for each lane group, which determine signal timing parameters and vehicle trajectories. The solutions are passed to the *DO* program to update Lagrangian multipliers. The convergence criteria are evaluated with calculating the difference between upper- and lower-bounds of *SSTTO* problem. Then the feasibility of signal timing parameters is checked. If the solutions are infeasible, the optimization problem *FP* is solved, which updates the optimal CAV and HV trajectories based on the feasible signal plan. If the solutions from Lagrangian relaxation are feasible, they are optimal solutions to the original problem and there is no need to solve *FP*. RHC implements the trajectory of CAVs in addition to signal timing plans at the first time step into the Vissim micro-simulator. Then, the Lagrangian multipliers will be updated from the last updated solutions of Lagrangian relaxation, and the planning horizon rolls one time step forward until the study period is finished.

V. Case Study

We applied the proposed solution technique to an isolated four-leg intersection with exclusive left-turn lanes, as shown in Fig. 4. It is assumed that vehicles are on the desired lane before arriving the intersection neighborhood. The detection range is 1000 ft before and after the intersection. The signal status is updated every two seconds, while vehicle acceleration, speed, and position are updated every 0.5 seconds. The prediction horizon of RHC is 20 seconds. More details are provided in Table II.

The STTO problem is solved for a 15-minute study period. Table III summarizes different scenarios tested in this study. For each scenario, six different market penetration rates of CAVs (i.e., 0%, 20%, 40%, 60%, 80% and 100%) are considered to evaluate the effects of cooperative signal timing and

TABLE II
CASE STUDY PARAMETERS

Parameters	Value
Desired speed (ft/s)	44
Maximum acceleration (ft/s^2)	6.5
Maximum deceleration (ft/s^2)	11.5
HV reaction time (s)	1
CAV reaction time (s)	0.1
Detection range (ft)	1000
Average length of the vehicles (ft)	13
Safety distance between following vehicles (ft)	12
Car-following parameter α_1	0.95
Car-following parameter α_2	0.25
Trajectory updating interval (s)	0.5
Signal updating interval (s)	2
Minimum green time for through movement (s)	12
Minimum green time for left turns (s)	6
Maximum green time for through movement (s)	60
Maximum green time for left turns (s)	20
Yellow time interval (s)	4
Planning time horizon (s)	20
Study period (min)	15

TABLE III
DEMAND PATTERNS IN STTO CASE STUDY

Scenario	East and Westbound		North and Southbound	
	Through demand ($veh/h/ln$)	Left-turn demand ($veh/h/ln$)	Through demand ($veh/h/ln$)	Left-turn demand ($veh/h/ln$)
1	500	100	500	100
2	600	120	600	120
3	750	150	750	150
4	900	180	900	180
5	900	180	750	150

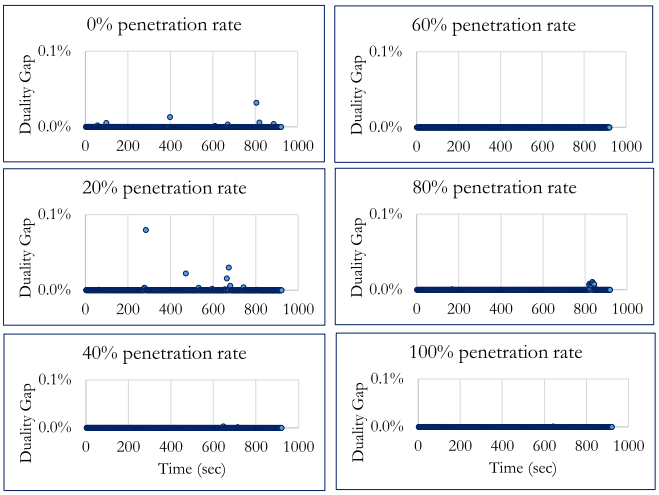

Fig. 6. Duality gaps for Lagrangian relaxation after reformulation.

TABLE IV
THE AVERAGE RUNTIME (S) FOR DIFFERENT SCENARIOS

CAV penetration rate	(1) Signal and trajectory optimization					(2) Trajectory optimization with fixed signal				
	Scenario									
	1	2	3	4	5	1	2	3	4	5
0%	3.2	3.9	5.2	5.9	5.5	0.10	0.12	0.19	0.22	0.20
20%	2.3	3.3	4.8	5.4	5.0	0.09	0.12	0.17	0.21	0.19
40%	1.8	2.7	3.5	4.1	3.7	0.08	0.10	0.14	0.17	0.15
60%	1.6	1.8	3.1	3.4	3.2	0.07	0.08	0.12	0.19	0.14
80%	1.3	1.4	2.2	2.8	2.4	0.05	0.07	0.12	0.13	0.12
100%	0.8	1.0	1.5	1.8	1.6	0.04	0.06	0.08	0.10	0.09

trajectory optimization planning. Vissim [45] is used to test the proposed algorithm. The COM interface is used to collect the information of vehicles in the network and apply the optimal trajectories to the motion of CAVs. The proposed algorithm is coded in Java running on a desktop computer with Intel core i-9-9900 CPU and 64 GB memory. CPLEX [46] is used to solve the MILP optimization problem.

VI. RESULTS

Fig. 6 shows the duality gaps in scenario 4, the highest demand level tested in this study, as a result of solving STTO problem with the proposed Lagrangian relaxation technique when pairwise conflicting constraints (13) are replaced with tighter cliques. Since the problem is solved through receding horizon control, the Lagrangian relaxation problem is solved every two seconds to find the optimal signal timing plans. Hence, the duality gaps are reported overtime for all relaxed problems that are solved dynamically. Fig. 6 indicates that the duality gap is mostly zero, meaning that the proposed solution technique mostly holds the strong duality. Moreover, it is shown that the duality gaps are always less than 0.1% in all cases tested with different CAV market penetration rates in scenario 4. Note that results for other scenarios also confirm the same patterns.

Table IV shows the average computational runtime of the proposed model for scenarios 1 to 5. The average runtime is shown for two optimization programs where (1) signal timing parameters and trajectories are optimized simultaneously, and (2) only trajectories are optimized with fixed signal timing parameters. In both cases, the optimization runtime decreases when CAV market penetration rate increases since the number of variables associated with car-following model of HVs decreases. It is also shown that increasing the traffic volume is associated with a higher runtime. The minimum and maximum average runtime for signal and trajectory optimization with enhanced Lagrangian relaxation technique was 0.8 s and 5.9 s, respectively. It should be noted that the proposed method is an iterative approach and might not find the optimal solution in real time since the signal timing parameters are optimized each 2s. However, real time solutions are achievable by setting the optimality gap to higher values or updating signal timing parameters in higher intervals. Table IV also shows that the minimum and maximum runtime for trajectory optimization with fixed signal parameters are 0.04 s and 0.22 s, respectively.

Table V compares the average travel time for different CAV market penetration rates of the STTO strategy with three state-of-practice signal control approaches: (a) fixed-time [47]–[49], (b) actuated, and (c) adaptive signal control. The fixed-time signal control can be seen as a baseline, where signal timing parameters are optimized based on a prediction on demand levels in different times of day. Fixed-time signal control is not responsive to unforeseen demand variations. The actuated control utilizes vehicle detectors and can react to changes in

TABLE V
AVERAGE TRAVEL TIME (S) FOR DIFFERENT SIGNAL CONTROLLERS

Scenario	Fixed-time signal	Actuated signal control	Adaptive signal control	STTO with different penetration rates					
				0%	20%	40%	60%	80%	100%
1	87.7	84.3	75.6	71.2	66.1	65.7	64.3	63.7	62.2
2	104.3	97.1	85.9	74.1	72.4	67.9	64.5	63.7	62.9
3	141.3	130.6	117.3	105.6	95.1	85.2	76.2	73.0	70.9
4	185.1	171.1	137.8	117.6	109.1	92.4	80.8	73.6	66.4
5	166.2	155.0	130.3	112.6	101.9	90.8	81.3	73.3	70.1

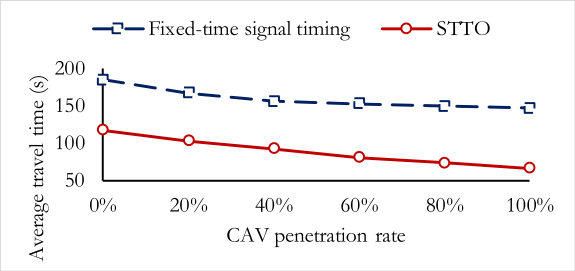

Fig. 7. Comparing the performance of STTO with fixed-time signal for various market penetration rate of CAVs.

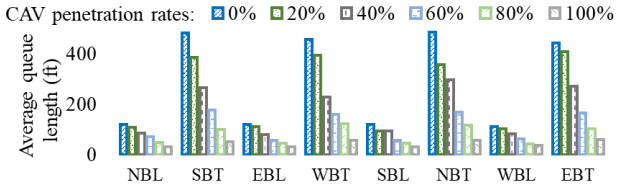

Fig. 8. Average queue length in scenario 4.

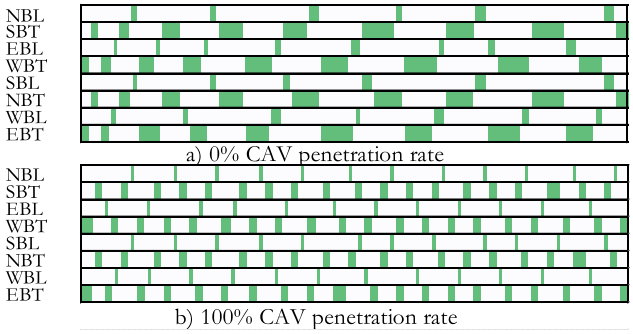

Fig. 9. Comparing signal timing plans under 0% and 100% CAV pen. rates.

traffic demand as they are observed. However, does not predict near future conditions. The adaptive signal control can predict traffic conditions in near future and can proactively change signal timing parameters. We used PTV Vistro [50] to find the optimal fixed-time and actuated signal timing plans. Moreover, the results of an adaptive signal control methodology based on the Cell Transmission Model [51]–[53] is provided for further comparisons.

The results show that STTO yields significantly shorter average travel time compared to the fixed time, actuated, and adaptive signal control in all scenarios with different CAV penetration rates. The results also show that the average travel time decreases as the CAV penetration rates increase, which is as expected. However, this reduction is less significant in low traffic volumes. For instance, the average travel time is almost the same when the CAV penetration rates are 60%, 80%, and 100% in scenarios 1 and 2. On the other hand, increasing the CAV penetration rate in scenarios with higher demand levels (e.g., scenario 4) still improves the performance of the intersection by reducing the average travel time of all vehicles. Moreover, we compared the performance of STTO with fixed-time signal timing plan when the market penetration rate of CAVs changes. Scenario 4 was considered for this analysis since it has the highest demand. When signal timing is fixed, only the trajectory of CAVs is optimized to utilize the green time efficiently and reduce the number of stops at the intersection. Fig. 7 shows that STTO always outperforms the fixed-time signal timing plan in terms if average travel time. In addition, the rate of decrease in travel time is higher with STTO compared to the fixed-time plan when the market penetration rate of CAVs increases.

Fig. 8 shows the average queue length in all movements in different approaches of the case study intersection with different CAV penetration rates in scenario 4, which has the highest tested demand level. The average queue length decreases with an increase in CAV market penetration rate. The average queue length is about 450 ft when there is no CAV on the road to control the movement of human-driven vehicles. The average queue length reduces to less than 50 ft when all vehicles are CAVs.

Fig. 9 shows the signal timing parameters for all movements in different approaches of the intersection with 0% and 100% CAV penetration rates in scenario 4 with the highest tested demand level. The green period for all movements of the intersection is longer when the CAV penetration rate is zero. This is due to the high start-up-lost time of human-driven vehicles. On the other hand, the green period is shorter and more frequent when all vehicles are CAVs. This is due to a low start-up lost time of CAVs when they are stopped before the intersection. Moreover, CAVs adjust their speed to pass the intersection with the maximum speed; hence, they require shorter green durations to pass the intersection.

Fig. 10 shows the trajectory of CAVs and HVs on east-bound through (EBT) for different market penetration rates in Scenario 4 with the highest tested demand. Increasing the penetration rate of CAVs is associated with a smoother trajectory for all vehicles to travel through the intersection. In addition, the back of the queue gets closer to the intersection as the market penetration rate of CAVs increase.

Since none of current state-of-practice strategies jointly optimize the signal timing plans with the trajectory of CAVs, we have compared the result of STTO with a recently developed state-of-art strategy in Guo *et al.* [3]. This study optimizes the signal timing plan and trajectory of CAVs in a mixed environment using dynamic programming and shooting heuristic. The findings show that the proposed algorithm in our

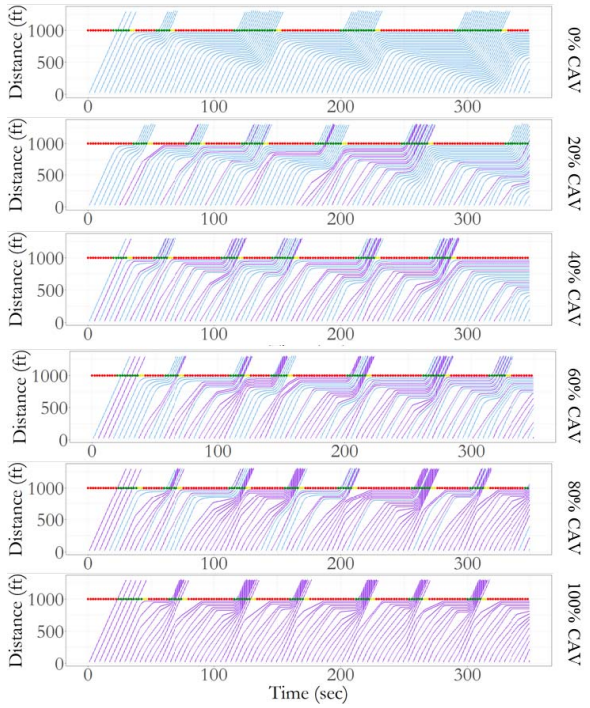

Fig. 10. The trajectory of CAVs and HVs in Lane 1.

TABLE VI
COMPARING WITH GUO ET AL. [4]

CAV Penetration rate	Average travel time (s)		Average fuel (lit/veh)	
	This study	Guo et al.	This study	Guo et al.
0%	72.81	114.10	0.150	0.180
20%	68.25	96.46	0.147	0.149
40%	65.29	75.06	0.145	0.146
60%	55.47	75.06	0.140	0.146
80%	49.49	75.06	0.123	0.146
100%	43.88	75.06	0.100	0.146

paper could find lower average travel time and fuel consumption with lower computational times. The fuel consumption is calculated based on VT-Micro model [54] with similar parameters to Ma *et al.* [55]. The following parameters are set exactly the same as the studied case in Guo *et al.* [3]: Length of intersection link: 1312 ft, Saturation rate f_s: 0.6, Maximum speed for through movement: 98 ft/s, Maximum speed for left turn movements: 79 ft/s, Planning horizon: 122 s, Car following parameter: maximum acceleration = 4.72 ft/S^2, maximum deceleration = 5.48 ft/S^2, and Step size to optimize signal timing plans: 8 seconds.

Table VI shows that the average travel time and fuel consumption is reduced by increasing the market penetration rate of CAVs. In addition, our proposed algorithm performs better than the best results in [3] for different market penetration rates of CAVs. It should be noted that Guo *et al.* [3] assumed that there are four phases for signal timing plans. However, our study includes eight phases, which represent a more general condition. Moreover, phases in [3] are considered in fixed order in a cycle even though some phases could be skipped. On the other hand, in our study, no order for phases are considered. Therefore, these differences in parameters could potentially affect the result of this comparison. All these differences created a larger feasible area for our problem, which led to the significant difference in the solution quality presented in Table VI.

TABLE VII
STTO PERFORMANCE WITH DIFFERENT STUDY PERIODS

Study period (min)	40 % CAV penetration rate			100 % CAV penetration rate		
	Average travel time (s)	Average fuel (lit/veh)	Total Runtime (min)	Average travel time (s)	Average fuel (lit/veh)	Total Runtime (min)
5	68.4	0.134	11.15	60.8	0.115	5.85
10	80.2	0.144	24.97	65.3	0.124	12.33
15	83.5	0.147	38.82	66.7	0.127	22.06
30	85.1	0.151	71.95	67.4	0.129	59.47

Table VII shows average travel time, average fuel consumption, and total runtime obtained by STTO for 5, 10, 15, and 30 minutes of study period. The performance measures are provided for scenario 4, which has the highest demand, and two CAV market penetration rates of 40% and 100%. The trends in Table VII shows that increasing the study period is associated with higher average travel time and average fuel consumptions due to presence of more vehicles in the network. In addition, the runtime increases by increasing the study period due to higher number of variables and memory usage.

VII. CONCLUSION

This study developed a methodology for coordinated signal timing and trajectory optimization at signalized intersections in a mixed traffic environment of CAVs and HVs. We formulated STTO as a mixed-integer nonlinear program assuming that either all vehicles were connected, or the intersection was equipped with detectors (e.g., radar units) that could provide location of vehicles. The trajectory of HVs were predicted using Helly's car-following model.

The proposed optimization program is complex due to nonlinearity and the presence of binary variables. Hence, we reduced the complexity of the problem by linearizing the nonlinear constraints and decomposing the interactable optimization problem into lane-level sub-problems using Lagrangian relaxation technique. Thus, the signal timing parameters and trajectory of vehicles in each lane of the intersection could be controlled with a single controller. We also reformulated STTO problem with a tight convex hull of the feasible area to reduce the duality gap. In addition, a complementary optimization problem was introduced to find high-quality feasible signal timing parameters when the relaxed constraints were not satisfied after the convergence of Lagrangian relaxation problem. The proposed solution technique was embedded in a receding horizon control technique to capture the dynamic nature of the problem.

The result shows that the developed methodology can find solutions within an optimality gap of at most 0.1% in the cases tested. It is also shown that STTO outperforms the

signal timing parameters found by an adaptive controller by decreasing the average travel time by 5% to 51% for different CAV market penetration rates tested in this study. Furthermore, increasing the penetration rate of CAVs reduces the average travel time for all vehicles at the intersection. This reduction is more significant in higher traffic volumes.

The proposed methodology is applicable to intersection layouts that operate left-turn movements exclusively. It will be worthwhile in the future to generalize the methodology and find optimal signal timing parameters and vehicles trajectory in all intersection types. In addition, this study assumed that vehicles do not change the lane within the detected range of intersection and did not use CAV lane change to further control the flow of traffic. Developing an algorithm for predicting the lane changing behavior of HVs and optimizing the lane changing decision of CAVs could further improve traffic operations. This study utilized a linear car following model and it is worthwhile to explore using more complex car fallowing models. Studying the effects of the signal timing and trajectory control in a transportation network, where intersections communicate and coordinate their decisions with each other offers great potential for further improvement in traffic operations and safety and needs to be studied.

REFERENCES

[1] C. Yu, Y. Feng, H. X. Liu, W. Ma, and X. Yang, "Integrated optimization of traffic signals and vehicle trajectories at isolated urban intersections," *Transp. Res. B, Methodol.*, vol. 112, pp. 89–112, Jun. 2018.

[2] K. Yang, S. I. Guler, and M. Menendez, "Isolated intersection control for various levels of vehicle technology: Conventional, connected, and automated vehicles," *Transp. Res. C, Emerg. Technol.*, vol. 72, pp. 109–129, Nov. 2016.

[3] Y. Guo, J. Ma, C. Xiong, X. Li, F. Zhou, and W. Hao, "Joint optimization of vehicle trajectories and intersection controllers with connected automated vehicles: Combined dynamic programming and shooting heuristic approach," *Transp. Res. C, Emerg. Technol.*, vol. 98, pp. 54–72, Jan. 2019.

[4] P. J. Li and X. Zhou, "Recasting and optimizing intersection automation as a connected-and-automated-vehicle (CAV) scheduling problem: A sequential branch- and-bound search approach in phase-time-traffic hypernetwork," *Transp. Res. B, Methodol.*, vol. 105, pp. 479–506, Nov. 2017.

[5] M. Tajalli, M. Mehrabipour, and A. Hajbabaie, "Network-level coordinated speed optimization and traffic light control for connected and automated vehicles," *IEEE Trans. Intell. Transp. Syst.*, early access, Jun. 5, 2020, doi: 10.1109/TITS.2020.2994468.

[6] R. Mohebifard, S. M. A. B. A. Islam, and A. Hajbabaie, "Cooperative traffic signal and perimeter control in semi-connected urban-street networks," *Transp. Res. C, Emerg. Technol.*, vol. 104, pp. 408–427, Jul. 2019.

[7] Z. Li, L. Elefteriadou, and S. Ranka, "Signal control optimization for automated vehicles at isolated signalized intersections," *Transp. Res. C, Emerg. Technol.*, vol. 49, pp. 1–18, Dec. 2014.

[8] H. Jung, S. Choi, B. B. Park, H. Lee, and S. H. Son, "Bi-level optimization for eco-traffic signal system," in *Proc. Int. Conf. Connected Vehicles Expo (ICCVE)*, Sep. 2016, pp. 29–35.

[9] B. Xu *et al.*, "Cooperative method of traffic signal optimization and speed control of connected vehicles at isolated intersections," *IEEE Trans. Intell. Transp. Syst.*, vol. 20, no. 4, pp. 1390–1403, Apr. 2019.

[10] P. Li, P. Mirchandani, and X. Zhou, "Solving simultaneous route guidance and traffic signal optimization problem using space-phase-time hypernetwork," *Transp. Res. B, Methodol.*, vol. 81, pp. 103–130, Nov. 2015.

[11] A. Mirheli, M. Tajalli, R. Mohebifard, L. Hajibabai, and A. Hajbabaie, "Utilization management of highway operations equipment," *Transp. Res. Rec.*, vol. 2674, no. 9, pp. 202–215, 2020.

[12] A. Mirheli and L. Hajibabai, "Utilization management and pricing of parking facilities under uncertain demand and user decisions," *IEEE Trans. Intell. Transp. Syst.*, vol. 21, no. 5, pp. 2167–2179, May 2020.

[13] W. Helly, "Simulation of bottlenecks in single lane traffic flow," in *Proc. Symp. Theory Traffic Flow*. New York, NY, USA: Research Laboratories, General Motors, 1959, pp. 207–238.

[14] M. Tajalli and A. Hajbabaie, "Dynamic speed harmonization in connected urban street networks," *Comput.-Aided Civil Infrastruct. Eng.*, vol. 33, no. 6, pp. 510–523, Jun. 2018.

[15] M. Tajalli and A. Hajbabaie, "Distributed optimization and coordination algorithms for dynamic speed optimization of connected and autonomous vehicles in urban street networks," *Transp. Res. C, Emerg. Technol.*, vol. 95, pp. 497–515, Oct. 2018.

[16] B. HomChaudhuri, A. Vahidi, and P. Pisu, "A fuel economic model predictive control strategy for a group of connected vehicles in urban roads," in *Proc. Amer. Control Conf. (ACC)*, Jul. 2015, pp. 2741–2746.

[17] X. He, H. X. Liu, and X. Liu, "Optimal vehicle speed trajectory on a signalized arterial with consideration of queue," *Transp. Res. C, Emerg. Technol.*, vol. 61, pp. 106–120, Dec. 2015.

[18] J. Misener, S. Shladover, and S. Dickey, "Investigating the potential benefits of broadcasted signal phase and timing (SPaT) data under IntelliDriveSM," presented at the ITS Amer. Annu. Meeting, Houston, TX, USA, 2010.

[19] H. Xia *et al.*, "Field operational testing of ECO-approach technology at a fixed-time signalized intersection," in *Proc. 15th Int. IEEE Conf. Intell. Transp. Syst.*, Sep. 2012, pp. 188–193.

[20] Y. Wei *et al.*, "Dynamic programming-based multi-vehicle longitudinal trajectory optimization with simplified car following models," *Transp. Res. B, Methodol.*, vol. 106, pp. 102–129, Dec. 2017.

[21] K. Dresner and P. Stone, "Multiagent traffic management: An improved intersection control mechanism," in *Proc. 4th Int. Joint Conf. Auto. Agents Multiagent Syst. (AAMAS)*, 2005, pp. 530–537.

[22] I. A. Zohdy and H. A. Rakha, "Intersection management via vehicle connectivity: The intersection cooperative adaptive cruise control system concept," *J. Intell. Transp. Syst.*, vol. 20, no. 1, pp. 17–32, 2016.

[23] A. Mirheli, L. Hajibabai, and A. Hajbabaie, "Development of a signal-head-free intersection control logic in a fully connected and autonomous vehicle environment," *Transp. Res. C, Emerg. Technol.*, vol. 92, pp. 412–425, Jul. 2018.

[24] C. Yu, Y. Feng, H. X. Liu, W. Ma, and X. Yang, "Corridor level cooperative trajectory optimization with connected and automated vehicles," *Transp. Res. C, Emerg. Technol.*, vol. 105, pp. 405–421, Aug. 2019.

[25] A. Mirheli, M. Tajalli, L. Hajibabai, and A. Hajbabaie, "A consensus-based distributed trajectory control in a signal-free intersection," *Transp. Res. C, Emerg. Technol.*, vol. 100, pp. 161–176, Mar. 2019.

[26] M. Pourmehrab, L. Elefteriadou, S. Ranka, and M. Martin-Gasulla, "Optimizing signalized intersections performance under conventional and automated vehicles traffic," *IEEE Trans. Intell. Transp. Syst.*, vol. 21, no. 7, pp. 2864–2873, Jul. 2020.

[27] Y. Feng, C. Yu, and H. X. Liu, "Spatiotemporal intersection control in a connected and automated vehicle environment," *Transp. Res. C, Emerg. Technol.*, vol. 89, pp. 364–383, Apr. 2018.

[28] M. Li, X. Wu, X. He, G. Yu, and Y. Wang, "An eco-driving system for electric vehicles with signal control under V2X environment," *Transp. Res. C, Emerg. Technol.*, vol. 93, pp. 335–350, Aug. 2018.

[29] R. Niroumand, M. Tajalli, L. Hajibabai, and A. Hajbabaie, "Joint optimization of vehicle-group trajectory and signal timing: Introducing the white phase for mixed-autonomy traffic stream," *Transp. Res. C, Emerg. Technol.*, vol. 116, Jul. 2020, Art. no. 102659.

[30] R. Niroumand, M. Tajalli, L. Hajibabai, and A. Hajbabaie, "The effects of the 'white phase' on intersection performance with mixed-autonomy traffic stream," in *Proc. IEEE 23rd Int. Conf. Intell. Transp. Syst. (ITSC)*, Sep. 2020, pp. 2795–2800.

[31] M. Wang, W. Daamen, S. P. Hoogendoorn, and B. van Arem, "Rolling horizon control framework for driver assistance systems. Part II: Cooperative sensing and cooperative control," *Transp. Res. C, Emerg. Technol.*, vol. 40, pp. 290–311, Mar. 2014.

[32] W. J. Schakel, B. van Arem, and B. D. Netten, "Effects of cooperative adaptive cruise control on traffic flow stability," in *Proc. 13th Int. IEEE Conf. Intell. Transp. Syst.*, Sep. 2010, pp. 759–764.

[33] S. Panwai and H. Dia, "Comparative evaluation of microscopic car-following behavior," *IEEE Trans. Intell. Transp. Syst.*, vol. 6, no. 3, pp. 314–325, Sep. 2005.

[34] M. Brackstone and M. McDonald, "Car-following: A historical review," *Transp. Res. F, Traffic Psychol. Behav.*, vol. 2, no. 4, pp. 181–196, Dec. 1999.

[35] A. Askari, D. A. Farias, A. A. Kurzhanskiy, and P. Varaiya, "Measuring impact of adaptive and cooperative adaptive cruise control on throughput of signalized intersections," 2016, *arXiv:1611.08973*. [Online]. Available: http://arxiv.org/abs/1611.08973
[36] L. Hajibabai and Y. Ouyang, "Integrated planning of supply chain networks and multimodal transportation infrastructure expansion: Model development and application to the biofuel industry," *Comput.-Aided Civil Infrastruct. Eng.*, vol. 28, no. 4, pp. 247–259, Apr. 2013.
[37] M. L. Fisher, "The Lagrangian relaxation method for solving integer programming problems," *Manage. Sci.*, vol. 27, no. 1, pp. 1–18, Jan. 1981.
[38] A. T. Murray and R. L. Church, "Analyzing cliques for imposing adjacency restrictions in forest models," *For. Sci.*, vol. 42, no. 2, pp. 166–175, 1996.
[39] A. T. Murray and R. L. Church, "Facets for node packing," *Eur. J. Oper. Res.*, vol. 101, no. 3, pp. 598–608, Sep. 1997.
[40] M. W. Padberg, "On the facial structure of set packing polyhedra," *Math. Program.*, vol. 5, no. 1, pp. 199–215, Dec. 1973.
[41] J. H. Kappes, B. Savchynskyy, and C. Schnorr, "A bundle approach to efficient MAP-inference by Lagrangian relaxation," in *Proc. IEEE Conf. Comput. Vis. Pattern Recognit.*, Jun. 2012, pp. 1688–1695.
[42] X. Zhao and P. B. Luh, "New bundle methods for solving Lagrangian relaxation dual problems," *J. Optim. Theory Appl.*, vol. 113, no. 2, pp. 373–397, May 2002.
[43] I. Nowak, *Relaxation and Decomposition Methods for Mixed Integer Nonlinear Programming*, vol. 152. Springer, 2005.
[44] K. C. Kiwiel, "Proximity control in bundle methods for convex nondifferentiable minimization," *Math. Program.*, vol. 46, nos. 1–3, pp. 105–122, Jan. 1990.
[45] *PTV Vissim 7 User Manual*, PTV Group, Karlsruhe, Germany, 2013.
[46] IBMI Complex, "V12. 1: User's manual for CPLEX," *Int. Bus. Mach. Corp.*, vol. 46, no. 53, p. 157, 2009.
[47] A. Hajbabaie, "Intelligent dynamic signal timing optimization program," Ph.D. dissertation, Dept. Civil Environ. Eng., Univ. Illinois Urbana-Champaign, Champaign, IL, USA, 2012.
[48] A. Hajbabaie and R. F. Benekohal, "Traffic signal timing optimization: Choosing the objective function," *Transp. Res. Rec., J. Transp. Res. Board*, vol. 2355, no. 1, pp. 10–19, Jan. 2013.
[49] A. Hajbabaie and R. F. Benekohal, "A program for simultaneous network signal timing optimization and traffic assignment," *IEEE Trans. Intell. Transp. Syst.*, vol. 16, no. 5, pp. 2573–2586, Oct. 2015.
[50] PTV Group, *PTV Vistro User Manual*, PTV AG, Karlsruhe, Germany, 2014.
[51] S. M. A. B. A. Islam and A. Hajbabaie, "Distributed coordinated signal timing optimization in connected transportation networks," *Transp. Res. C, Emerg. Technol.*, vol. 80, pp. 272–285, Jul. 2017.
[52] S. M. A. B. A. Islam, H. M. A. Aziz, and A. Hajbabaie, "Stochastic gradient-based optimal signal control with energy consumption bounds," *IEEE Trans. Intell. Transp. Syst.*, early access, Mar. 18, 2020, doi: 10.1109/TITS.2020.2979384.
[53] S. M. A. B. A. Islam, A. Hajbabaie, and H. M. A. Aziz, "A real-time network-level traffic signal control methodology with partial connected vehicle information," *Transp. Res. C, Emerg. Technol.*, vol. 121, Dec. 2020, Art. no. 102830.
[54] K. Ahn, H. A. Rakha, and S. Park, "Ecodrive application: Algorithmic development and preliminary testing," *Transp. Res. Rec., J. Transp. Res. Board*, vol. 2341, no. 1, pp. 1–11, Jan. 2013.
[55] J. Ma, X. Li, F. Zhou, J. Hu, and B. B. Park, "Parsimonious shooting heuristic for trajectory design of connected automated traffic part II: Computational issues and optimization," *Transp. Res. B, Methodol.*, vol. 95, pp. 421–441, Jan. 2017.

Mehrdad Tajalli (Member, IEEE) received the B.Sc. degree in civil engineering from the Iran University of Science and Technology, Tehran, Iran, in 2011, and the M.Sc. degree in civil engineering from the Sharif University of Technology, Tehran, in 2014. He is currently pursuing the Ph.D. degree with the Department of Civil, Construction, and Environmental Engineering, North Carolina State University. His research interests include network optimization, speed harmonization, and safety.

Ali Hajbabaie (Member, IEEE) received the B.S. and M.S. degrees from the Sharif University of Technology, Tehran, Iran, in 2003 and 2006, respectively, and the M.S. degree in industrial engineering and the Ph.D. degree in civil engineering from the University of Illinois at Urbana–Champaign in 2011 and 2012, respectively. He is currently an Assistant Professor with the Department of Civil, Construction, and Environmental Engineering, North Carolina State University. His research interests include traffic operations and control, connected and automated vehicles, distributed optimization, and traffic flow theory. He was a recipient of the Junior Outstanding Researcher from the Department of Civil and Environmental Engineering, Washington State University.